Antarctic Science 7 (2): 199–210 (1995)

A case study of a midtropospheric subsynoptic-scale cyclone that developed over the Ross Sea and Ross Ice Shelf of Antarctica

JORGE F. CARRASCO[1] and DAVID H. BROMWICH

Polar Meteorology Group, Byrd Polar Research Center and Atmospheric Sciences Program, The Ohio State University, Columbus, Ohio 43210, USA

[1]Permanent Affiliation: Direccion Meteorologica de Chile, Santiago, Chile

Abstract: Satellite imagery, synoptic-scale analyses and automatic weather station data were used to study a subsynoptic-scale cyclone that developed over the Ross Sea and Ross Ice Shelf areas of Antarctica. A pre-existing subsynoptic-scale midtropospheric cyclone descended from southern Victoria Land into the semi-permanent baroclinic environment over the south-western corner of the Ross Sea. The subsynoptic-scale cyclone then developed into a frontal system travelling south-eastward over the Ross Ice Shelf and decayed five days later over Marie Byrd Land. It is concluded that stretching of the subsynoptic-scale low, while descending over 2000 m from the high plateau down to sea level, increased its cyclonic vorticity via conservation of potential vorticity. This, along with a cold katabatic outbreak into the northern part of the circulation, provided the mechanisms for its initial development. Subsequently, cold boundary-layer air over the Ross Ice Shelf spiralled into the subsynoptic-scale cyclone supporting its further development. An upper-level synoptic-scale cyclone that approached the area provided the upper-level support for its ESE displacement and development.

Received 25 January 1994, accepted 28 November 1994

Key words: katabatic winds, mesoscale cyclogenesis, potential vorticity, warm/cold air advection

Introduction

The Southern Hemisphere has a belt of low pressure at sea level that surrounds the Antarctic continent (van Loon 1972, Schwerdtfeger 1984). This circumpolar trough represents the area where mature synoptic-scale cyclones decay near Antarctica. Within the circumpolar trough, four low pressure centres are the preferred regions for synoptic-scale cyclolysis (e.g. Streten & Troup 1973). One of these centres is located to the north-east of the Ross Sea/Ross Ice Shelf area (Fig. 1), giving this region a semi-permanent cyclonic circulation. The deployment of automatic weather stations (AWS) over the Ross Sea/Ross Ice Shelf area since 1980 by the US Antarctic Program (Stearns & Wendler 1988) has resulted in the regional climatology being better defined. In addition to the average synoptic-scale cyclonic circulation, the regional analysis shows subsynoptic-scale troughs and ridges along the Transantarctic Mountains. One sea-level pressure trough is present over the south-western corner of the Ross Sea (Bromwich 1991, Bromwich *et al.* 1993).

Observational and numerical studies of the near-surface wind regime over the Antarctic continent and in particular near Terra Nova Bay (Bromwich 1989a, Bromwich *et al.* 1990, Bromwich *et al.* 1993, Parish & Bromwich 1987, 1989, 1991) show that the winds converge into Reeves and David glaciers and then blow offshore over the south-western Ross Sea. These katabatic winds are intensified and more persistent due to the large supply of negatively buoyant air from the continental interior resulting from this convergence.

Bromwich (1991) through the study of two years (1984–85) of combined AWS data and satellite imagery found that, on average, 1–2 subsynoptic-scale (or mesoscale) cyclones (diameter typically less than 5×10^2 km) form over the south-western corner of the Ross Sea. Later, Carrasco & Bromwich (1994) obtained similar results from the study of an additional year (1988), confirming this area as a very active region for mesoscale cyclogenesis. The subsynoptic-scale surface pressure trough reflects the frequent mesoscale cyclonic activity in this area.

Individual case studies (Bromwich 1987, 1989b, 1991, Carrasco & Bromwich 1993) have shown that a subsynoptic surface trough and a katabatic outbreak provide sufficient conditions for mesoscale cyclogenesis near Terra Nova Bay. Therefore, these conditions which are frequently present over the south-western Ross Sea, make this area a semi-permanent baroclinic environment, where mesoscale cyclones can form. In addition, this baroclinic environment can intensify weak or dissipating subsynoptic-scale perturbations that move into the area. Here, an example of the latter is discussed. All available meteorological data are used to describe the subsynoptic- and synoptic-scale environments present at the time of formation and during subsequent evolution of a subsynoptic-scale vortex.

Mesoscale cyclogenesis

Satellite detection

Satellite images show that a well-defined subsynoptic frontal cyclone developed over the Ross Ice Shelf between 8 and 10 January 1988. Fig. 2a–e shows the NOAA AVHRR satellite images for January 7–10 collected at McMurdo Station on Ross

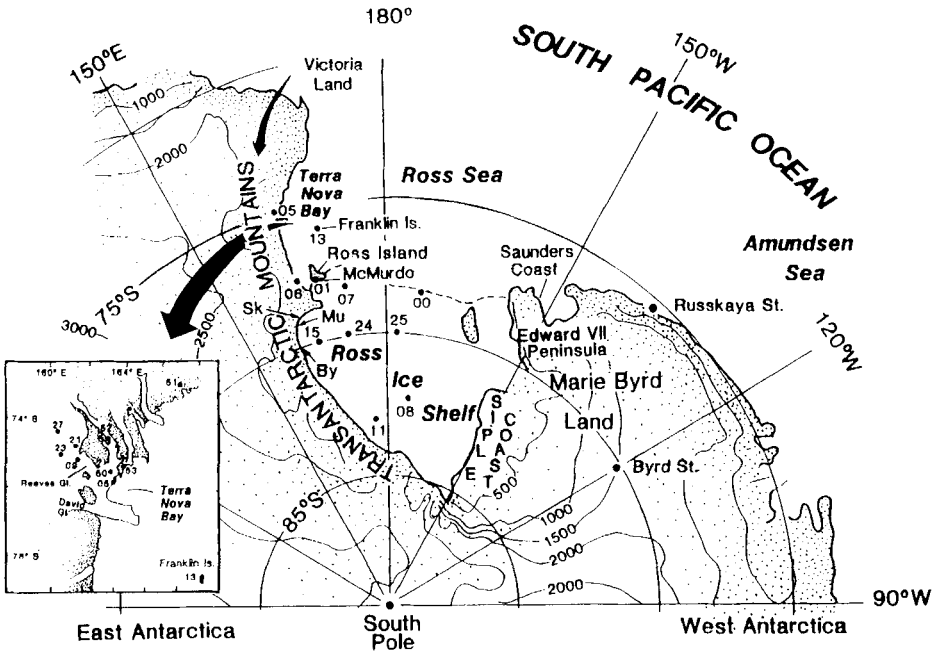

Fig. 1. Location map of the Ross Sea, Ross Ice Shelf and Victoria Land areas. The numbered dots are AWS sites. Big arrow points to the close up of the Terra Nova Bay area. Sk, Mu and By respectively identify Skelton, Mulock and Byrd glaciers.

Island (see Van Woert *et al.* 1992). The evolution of the cloud signature associated with the subsynoptic cyclone (L_1) is shown in Fig. 2b–e. The satellite image at 0339 UTC 8 January (Fig. 2b) shows a series of mesoscale vortices over the Ross Sea and Ross Ice Shelf. At this time L_1 (a comma cloud vortex according to its appearance in the satellite image) was already located to the north-east of Ross Island. Also, a weak comma vortex (L_2) is present near Byrd Glacier, and another (L_3) near the centre of the Ross Ice Shelf whose comma tail extends northward to merge with the cloud signature associated with L_1. A fourth mesoscale comma vortex can be observed to the north of L_1 whose comma-cloud head merges with L_1. Lastly, a fifth mesoscale system (L_5, a merry-go-round, a system formed by small vortices) is located to the east of L_1 over the Ross Sea.

Unfortunately, the satellite image ten hours earlier at 1715 UTC 7 January did not resolve the origin of these vortices. However, the satellite image at 0711 UTC 7 January (Fig. 2a) shows low cloud features spread out over the Ross Sea and Ross Ice Shelf. They have cyclonic appearance and seem to be part of a decaying synoptic-scale system although no clear evidence was found in the Australian Southern Hemisphere surface analyses, nor in the previous available satellite image (about 24 h earlier). A hook of middle/high cloud at 78°S, 170°W indicates the centre of this cyclone (Fig. 2a). The dissipating system could have been the source for L_2, L_3, L_4 and L_5, as well as providing the cloud that later was associated with L_1.

The satellite image at 1653 UTC 8 January (Fig. 2c) indicates that the system L_1–L_4 had moved toward the south-east over the Ross Ice Shelf. At this time, L_4 seems to have merged into L_1, and only a weak cloud signature can be associated with L_3 revealing its rapid weakening as L1 developed and moved south-eastward. L_2 had moved slightly toward the north, while L_5 had moved north-eastward and weakened. The next satellite images at 0509 UTC 9 January and 0639 UTC 10 January (Fig. 2d & e) show that L_1 became the dominant feature over the Ross Sea and Ross Ice Shelf. Therefore, the development of L_1 is emphasized hereafter. However, it is notable that the weak, small and shallow system, L_2, spiralled around the centre of L_1.

Synoptic-scale analyses

To study the synoptic-scale pattern in which the subsynoptic-scale cyclone developed, the sea-level pressure and 500 hPa Southern Hemisphere analyses produced by the Australian Bureau of Meteorology were examined. Fig. 3a–h are reproductions (every 24 h) of the hand-drawn synoptic sea-level pressure charts from 1200 UTC 7 January to 1200 UTC 14 January 1988. They were slightly modified, when necessary, over the Ross Sea/Ross Ice Shelf area to accord with the AWS data. At 1200 UTC 7 January, the analysis shows an anticyclonic circulation that affected most of the Ross Ice Shelf until 0000 UTC 8 January, and cyclonic circulation to the north of the Ross Sea, which was associated with synoptic-scale storms travelling eastward over the South Pacific Ocean. Later, a surface trough over the Ross Sea/Ross Ice Shelf between 1200 UTC 8 January and 1200 UTC 10 January (Fig. 3b–d) appears as the only manifestation of the subsynoptic scale cyclone that developed in this area (Fig. 2d–e).

The prevailing synoptic-scale midtropospheric circulation during formation and development of the subsynoptic-scale cyclone L_1 is shown by using the Australian numerical 500-hPa geopotential height analyses (Guymer 1986). The analyses are partially reproduced every 24 h from 1200 UTC 7 January to 1200 UTC 14 January in Fig. 4a–h, although previous analyses were also examined. The original analyses were slightly adjusted by incorporating 500 hPa heights estimated from the

https://doi.org/10.1017/S0954102095000277 Published online by Cambridge University Press

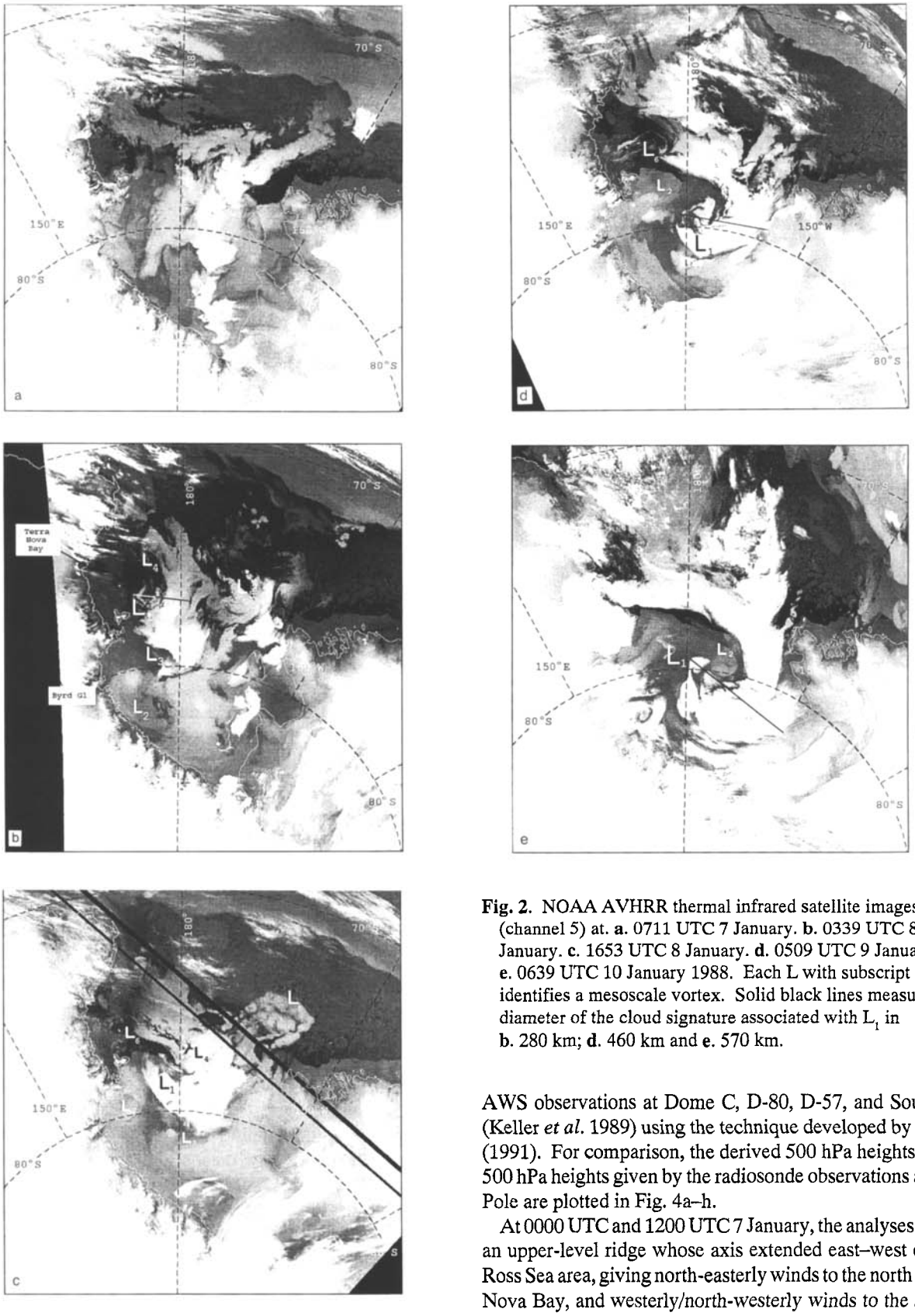

Fig. 2. NOAA AVHRR thermal infrared satellite images (channel 5) at. **a.** 0711 UTC 7 January. **b.** 0339 UTC 8 January. **c.** 1653 UTC 8 January. **d.** 0509 UTC 9 January **e.** 0639 UTC 10 January 1988. Each L with subscript number identifies a mesoscale vortex. Solid black lines measure the diameter of the cloud signature associated with L_1 in **b.** 280 km; **d.** 460 km and **e.** 570 km.

AWS observations at Dome C, D-80, D-57, and South Pole (Keller *et al.* 1989) using the technique developed by Phillpot (1991). For comparison, the derived 500 hPa heights and the 500 hPa heights given by the radiosonde observations at South Pole are plotted in Fig. 4a–h.

At 0000 UTC and 1200 UTC 7 January, the analyses showed an upper-level ridge whose axis extended east–west over the Ross Sea area, giving north-easterly winds to the north of Terra Nova Bay, and westerly/north-westerly winds to the south as

https://doi.org/10.1017/S0954102095000277 Published online by Cambridge University Press

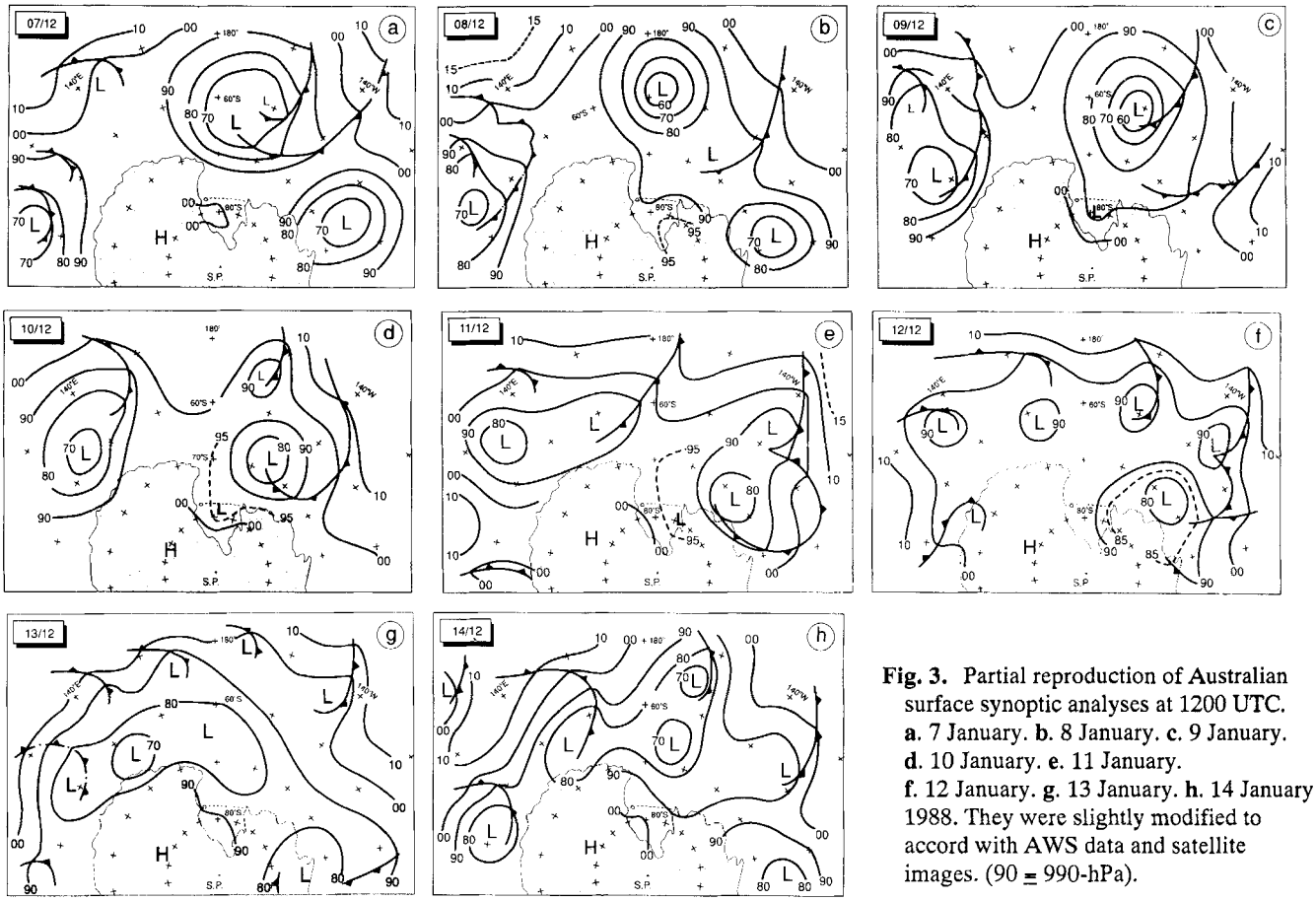

Fig. 3. Partial reproduction of Australian surface synoptic analyses at 1200 UTC. **a.** 7 January. **b.** 8 January. **c.** 9 January. **d.** 10 January. **e.** 11 January. **f.** 12 January. **g.** 13 January. **h.** 14 January 1988. They were slightly modified to accord with AWS data and satellite images. (90 = 990-hPa).

shown by the radiosonde at McMurdo Station on Ross Island. Also, the 500 hPa fields resolved an upper-level synoptic-scale cyclone over the plateau to the south of Ross Island (labelled Lg in Fig. 4). According to previous 500 hPa analyses, a low geopotential height centre at 500 hPa was resolved over Ross Island at 1200 UTC 5 January. This centre moved toward the SSE and south-west being located to the south of Ross Island as centre Lg at 0000 UTC 7 January (see Fig. 4a). At this time, and later at 1200 UTC 7 January, the 500 hPa analyses also resolved another low geopotential height centre just to the south-west of Ross Island over southern Victoria Land. This low (labelled Ls in Fig. 4a), which seems to be a subsynoptic-scale feature, was not shown on the 500 hPa analyses from 0000 UTC 8 January onward. However as will be seen, this is the first indication of L_1. For better identification Fig. 5 shows the location of both synoptic- and subsynoptic-scale cyclones as resolved by the Australian 500 hPa numerical analysis at 1200 UTC 7 January (Fig. 4a). Trajectories of both cyclones are also indicated.

The following analyses at 0000 UTC and 1200 UTC 8 January (Fig. 4b) indicate that the upper-level ridge retreated toward the north-east, and that the upper-level synoptic-scale cyclone Lg moved slightly closer to Ross Island. It remained nearly stationary over the plateau, to the south-west of Ross Island, until 1200 UTC 10 January (Fig. 4d). The 500 hPa analysis from 1200 UTC 11 January shows that the upper-level synoptic-scale cyclone (Lg) had moved to the north of Ross Island (Fig. 5). Later, over Wilkes Land, it merged with another upper-level synoptic cyclone coming from the north-west (Fig. 4e–h). On the other hand, the decrease of the geopotential height from 516 gpdam at 1200 UTC 7 January to 509 gpdam at 0000 UTC 8 January, and the clockwise rotation of the wind direction recorded at McMurdo Station, is associated with the displacement of the subsynoptic-scale low (Ls) near Ross Island.

Mesoscale analyses

Back tracking the trajectory of L_1 according to the satellite images at 0339 UTC and 1653 UTC 8 January, suggests that this vortex moved from the vicinity of Terra Nova Bay. The subsynoptic-scale low (Ls) resolved by the 500 hPa analyses approximately concurs with the probable position of L_1 inferred from the satellite images. However no indication of this vortex was observed on the satellite image at 0711 UTC 7 January (Fig. 2a). Three-hourly mesoscale surface charts were constructed from 0000 UTC 7 January to 1200 UTC 13 January to determine from sea-level pressure analyses the surface manifestation of the subsynoptic-scale low (Ls), and its subsequent development. Although the sea-level pressure started to decrease over the Ross Sea and Ross Ice Shelf from 0000 UTC 7 January, the surface analyses did not suggest a well-defined cyclonic

https://doi.org/10.1017/S0954102095000277 Published online by Cambridge University Press

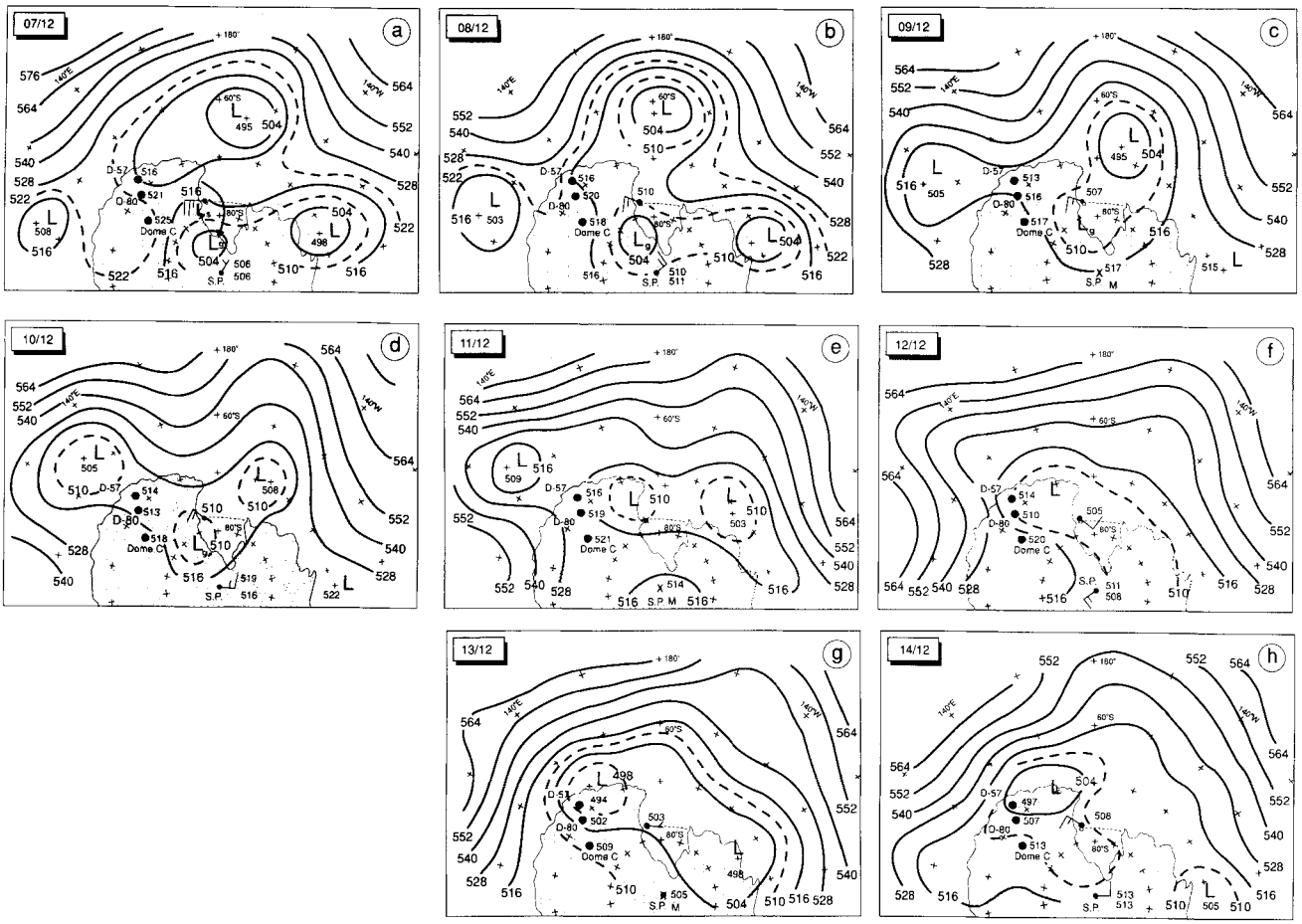

Fig. 4. Partial reproduction of Australian 500 hPa analyses at 1200 UTC. **a.** 7 January. **b.** 8 January. **c.** 9 January. **d.** 10 January. **e.** 11 January. **f.** 12 January. **g.** 13 January. **h.** 14 January 1988. At South Pole Station the estimated 500 hPa geopotential heights from AWS are plotted above the radiosonde-derived value (510 ≡ 5100 gpm). The radiosonde 500 hPa winds and geopotential heights at McMurdo and Pole stations are plotted when available in conventional format. Solid-black arrow in panel (a) indicates the movement of the synoptic-scale upper-level cyclone from 1200 UTC 5 January when it was first resolved by the analyses. Lg and Ls respectively identify the upper-level synoptic-scale cyclone and the subsynoptic-scale low.

circulation over Terra Nova Bay/Franklin Island area until 1500 UTC 7 January. Fig. 6a–d are respectively the sea-level regional analyses at 1800 UTC 7 January, 1200 UTC 8 January, 0600 UTC 9 January and 0600 UTC 10 January showing the pressure field associated with the evolution of L_1. Surface analysis at 1800 UTC 7 January (Fig. 6a) clearly resolves the cyclonic circulation over the Terra Nova Bay/Franklin Island area, and another much weaker one along the Transantarctic Mountains near Byrd Glacier. Both subsynoptic-scale cyclonic circulations are the surface manifestations of L_1 and L_2. No indication of L_3 or L_5 was detected from the AWS analyses indicating the weakness of these systems. Also, the analysis at 1800 UTC 7 January (Fig. 6a) better resolved the area of high pressure affecting the centre of the Ross Ice Shelf shown previously by the surface synoptic-scale analysis (Fig. 3a). This high pressure area weakened and moved eastward according to subsequent AWS regional analyses.

Negative (or minimum) sea-level pressure differences between Inexpressible and Franklin islands, and a relatively small difference in potential temperature between the sites along with a north–north-westerly wind at Franklin Island are usually associated with formation of mesoscale cyclones near Terra Nova Bay (e.g. Bromwich 1987, Carrasco & Bromwich 1993). These parameters are used to determine if there was a cyclogenesis event near Terra Nova Bay in conjunction with the approach of the subsynoptic-scale low (Ls). They are shown in Fig. 7 for the period between 0000 UTC 7 January and 0000 UTC 10 January 1988. The comparison does not reveal the characteristic signals in sea-level pressure and potential temperature differences associated with cyclogenesis over the south-western Ross Sea suggesting that the surface subsynoptic-scale cyclone resolved by the AWS data did not form in this area. Next, pressure field anomalies were constructed every three hours from 1200 UTC 6 January to 1200 UTC 8 January, to further clarify whether this cyclone actually formed near Terra Nova Bay or whether it was a pre-existing cyclonic perturbation that moved into the area and redeveloped. The anomalies correspond to the difference between the station pressure at chart time and the average for

https://doi.org/10.1017/S0954102095000277 Published online by Cambridge University Press

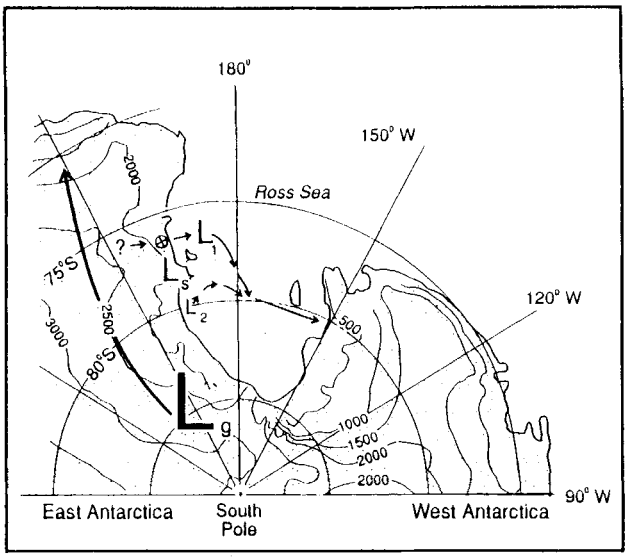

Fig. 5. Location of the subsynoptic and synoptic-scale upper level cyclones (Ls and Lg respectively) as resolved by the Australian 500 hPa numerical analysis at 1200 UTC 7 January. ⊗indicates the surface position of Ls over southern Victoria Land. L_1 denotes the position of Ls over the Ross Sea at 0339 UTC 8 January (Fig. 2b). L_2 is a mesoscale cyclone near Byrd Glacier. Arrows indicate the trajectories of the cyclones.

January 1988; they are a simple way of removing the large elevation differences between AWS sites and have been found to be effective for resolving small cyclones inland of Terra Nova Bay (Bromwich & Parish 1988, Carrasco & Bromwich 1993). Also, the potential temperature, wind direction and wind speed were analysed in conjunction with the pressure anomalies. Fig. 8a–g shows the pressure anomaly and potential temperature analyses every six hours from 0300 UTC 7 January to 0900 UTC 8 January over Victoria Land and the south-western corner of the Ross Sea. The analyses indicate that a relatively high pressure area affected the south-western corner of the Ross Sea, which started to retreat toward the north-east from 0300 UTC 7 January. In addition, a relatively low pressure area appeared to move from southern Victoria Land onto the south-western corner of the Ross Sea around 0900 UTC 7 January. From these results it is concluded that L_1 did not form near Terra Nova Bay, but it was a pre-existing perturbation that came down from the plateau. The relatively low pressure resolved by the pressure anomalies is the manifestation of the subsynoptic-scale vortex Ls observed at 500 hPa on 7 January (Fig. 4a). Therefore, Ls and L_1 identify the same feature, a midtropospheric subsynoptic-scale low (hereafter identified as L_1). Note that the surface manifestation of L_1 is centred slightly to the north of its position at 500 hPa, an indication of a slight southward tilt. The origin of this low, prior to its first identification over southern Victoria Land, cannot be determined from the available data. It is possible that it was a short-wave trough travelling around the synoptic-scale cyclone located over the plateau (Lg), or a subsynoptic-scale cyclonic perturbation coming from the north-west of the Terra Nova Bay/Franklin Island area.

As the relatively low pressure anomaly moved over the south-western corner of the Ross Sea around 0900 UTC 7 January, the katabatic wind at Reeves Glacier (as recorded by AWS 09 and AWS 05) increased and acquired a north-westerly direction (Fig. 7, also compare Fig. 8a, b & c). The potential temperature analyses suggest a cold air outbreak onto Terra Nova Bay that seems to have occurred from 0900 UTC 7 January onward (see Fig. 7 & Fig. 8b–c). This reveals the katabatic characteristics of the wind at Reeves Glacier. This katabatic airflow was probably supported by the cyclonic circulation associated with the incoming cyclone (Ls), and it reached maximum intensity at 0300 UTC 8 January. The temporary N–NE wind recorded at AWS 06 between 0000 UTC and 0900 UTC 7 January signals the passage of L_1 to the north of this site. From the pressure anomaly analyses, the centre of the subsynoptic-scale cyclone arrived over the south-western corner of the Ross Sea around 2100 UTC 7 January (Fig. 8d, see also Fig. 6a). The weak north-easterly wind experienced by AWS 07 from 0600 UTC to 2100 UTC 7 January and the south-easterly winds between 0300 UTC and 0900 UTC 8 January, indicate the continuing eastward movement of L_1 to the north of this site. The available data suggest that the cyclone was a sub-synoptic feature. According to the cloud signature associated with it at 0339 UTC 8 January, its diameter was around 280 km and the cloud-top temperatures ranged between -17 and -20°C. Unfortunately radiosonde data are not available for this case. At 0000 and 1200 UTC 8 January the air temperature was -35°C at 500 hPa. This is 15–18 degrees colder than the cloud-top temperatures. These temperatures suggest that the vortex was shallow at this time (below the 700 hPa level).

Cyclogenesis mechanisms associated with L_1

The above discussion leads to the conclusion that L_1 was a weak subsynoptic-scale midtropospheric cyclone coming from the plateau that developed (or redeveloped) once it arrived in the Terra Nova Bay/Franklin Island area. Fig. 9 schematically illustrates the two possible mechanisms which could be involved with the development of this cyclone. Firstly, assuming that the vortex behaves as a cylindrical column of air that descends adiabatically from the plateau, it stretches vertically and increases the cyclonic vorticity by conservation of potential vorticity (e.g. Holton 1992, p. 97–99). Unfortunately, the limited available data preclude a precise evaluation of this. However, scaling calculations were done using the potential vorticity equation, and the term $-\partial\theta/\partial p$ in Ertel's potential vorticity (Holton 1992, p. 98, Bluestein 1992, p. 380) to evaluate the increase in relative vorticity (ζ) as the midtropospheric subsynoptic-scale cyclone descended to the Ross Sea. Data from AWS 09 and AWS 13 were respectively used over Victoria Land and the western Ross Sea, and the McMurdo radiosonde temperature at 500 hPa was assumed to be representative of both areas. Evaluation indicated that the ζ increased by about $-8\times10^{-5}\,s^{-1}$ as the subsynoptic-scale

https://doi.org/10.1017/S0954102095000277 Published online by Cambridge University Press

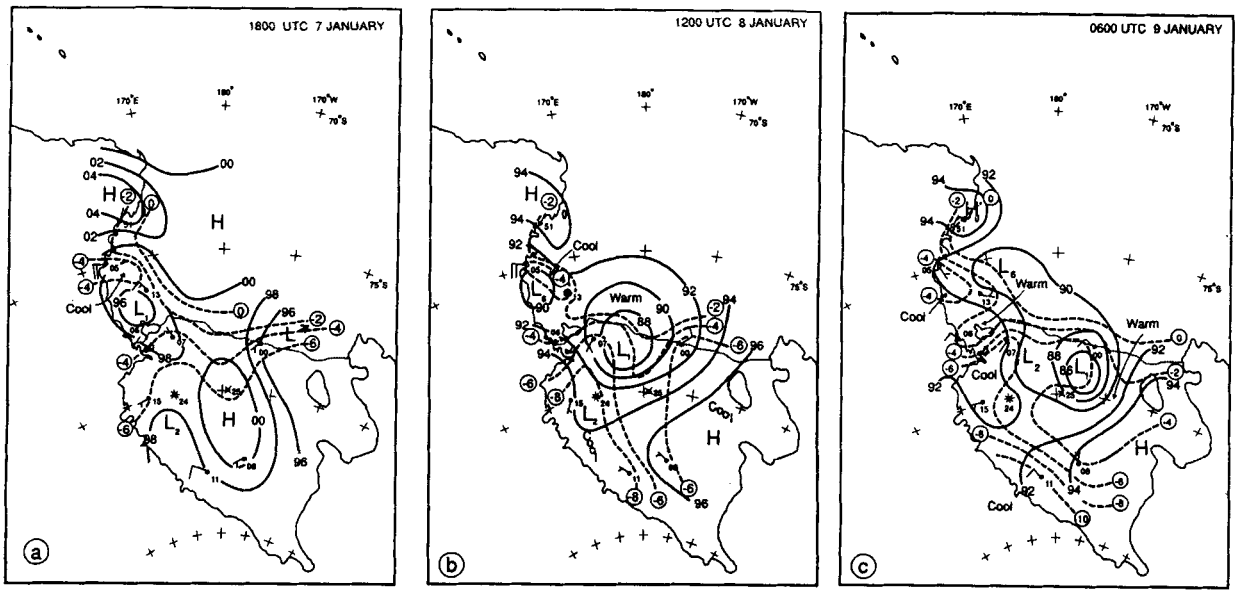

Fig. 6. Regional AWS sea-level pressure analyses at. **a.** 1800 UTC 7 January. **b.** 1200 UTC 8 January. **c.** 0600 UTC 9 January. **d.** 0600 UTC 10 January 1988. Sea-level isobars are solid lines every 2 hPa (90 = 990 hPa), and surface isotherms in degrees Celsius and are dashed every 2°C.

cyclone moved downward onto the Ross Sea. Secondly, a katabatic outbreak that developed while L_1 was passing to the south of Terra Nova Bay supplied cold boundary-layer air to the north side of the now developing subsynoptic-scale cyclone. This cold air could have interacted with the warmer air of the Ross Sea creating or enhancing a baroclinic front-like zone. These two mechanisms seem to occur almost simultaneously.

Additional scaling calculation of the radius of curvature (R_s) of the flow over southern Victoria Land was evaluated using the relative vorticity:

$$\zeta = \partial V/\partial n + V/R_s$$

where the first term is the rate of change of wind speed normal to the direction of flow (called the shear vorticity), and the second term is the turning of the wind along a streamline (called the curvature vorticity). Neglecting the shear vorticity and obtaining V by averaging the surface wind speed at Franklin Island (AWS 13) and the 500 hPa wind speed at McMurdo, we have $\zeta = V/R_s$. Calculations indicate that the radius of curvature of the flow was around 150 km suggesting that the diameter of the subsynoptic-scale perturbation was around 300 km, close to that inferable from Fig. 8c & d.

The upper-level circulation shown by the 500 hPa analyses, was dominated by the synoptic-scale cyclone (Lg) providing westerly and north-westerly flow over the Ross Sea/Ross Ice Shelf area that could have steered the subsynoptic-scale cyclone down from the plateau to the Ross Sea and then toward Marie Byrd Land. In addition in Fig. 9, L_2, L_3, L_4 and L_5 are portrayed as minor decaying perturbations in comparison to L_1.

Classical cyclogenesis at Terra Nova Bay

The three-hourly sea-level pressure and pressure anomaly analyses showed that in spite of the eastward movement of L_1, an area of lower pressure remained near Terra Nova Bay (Fig. 8d, e, & f). The acceleration of the katabatic winds from 0900 UTC 7 January to 0300 UTC 8 January that supported the development of L_1, could also have provided cold air for creation of a baroclinic zone near Terra Nova Bay. Minimum sea-level pressure differences between Inexpressible and Franklin islands from 0900 UTC to 1200 UTC 8 January, and a minimal potential temperature difference between the above sites at 0900 UTC 8 January (Fig. 7) that occurred after the maximum wind acceleration reveal the characteristic signals associated with cyclogenesis near Terra Nova Bay (e.g. Bromwich 1987, Carrasco & Bromwich 1993). This seems to have occurred at around 0900 UTC 8 January (Fig. 8f). The surface analysis at 1200 UTC 8 January (Fig. 6b) already resolved this cyclone just to the

https://doi.org/10.1017/S0954102095000277 Published online by Cambridge University Press

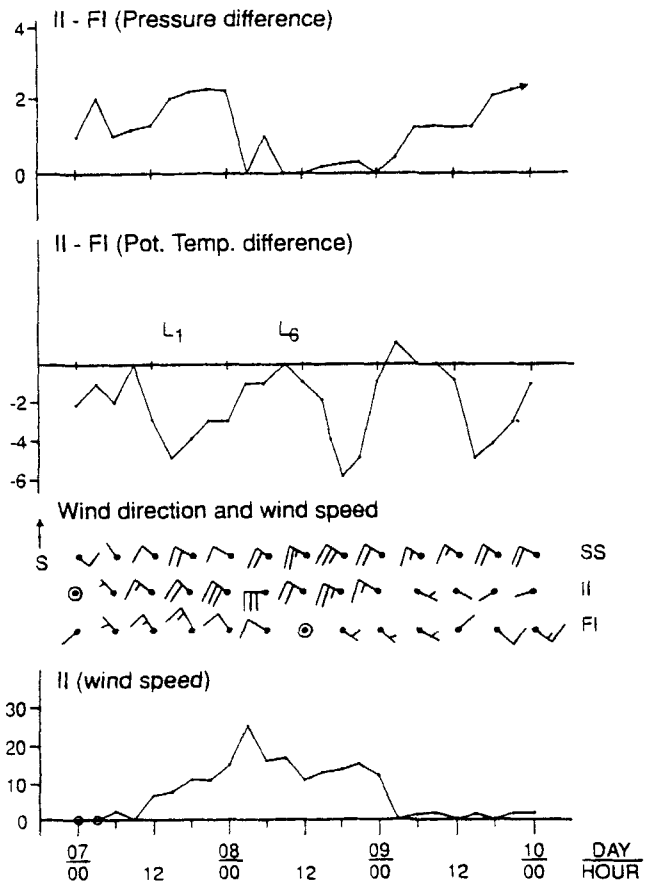

Fig. 7. Time series of the differences in sea-level pressure and potential temperature between Inexpressible Island (AWS 05) and Franklin Island (AWS 13). Also plotted are the wind speed and direction at both stations and at Shristi Station (AWS 09).

south of Terra Nova Bay, and later the satellite image at 1653 UTC 8 January (Fig. 2c) shows a weak comma-cloud feature just to the east of Franklin Island that may be the remnant of this cyclone (labelled L_6 in Fig. 2). The approach of the upper-level synoptic-scale cyclone, Lg, toward Ross Island could have supported the formation of this mesoscale cyclone by advecting cyclonic vorticity over the area (Bromwich 1991, Carrasco & Bromwich 1993). Fig. 10 schematically illustrates the mechanisms involved in the formation of L_6, i.e. a weak surface subsynoptic-scale trough over the south-western corner of the Ross Sea and a katabatic wind outbreak from Terra Nova Bay (Bromwich 1989b).

Subsequent development of L_1

The satellite image at 0509 UTC 9 January shows (Fig. 2d) a well-defined subsynoptic-scale cyclone over the Ross Ice Shelf. At this time, its diameter was around 460 km and the cloud-top temperatures range between -27 and -30°C on the comma head, and between -11 and -20°C on the tail. This reveals vertical development of the subsynoptic-scale cyclone (L_1). The sea-level pressure analysis at 0600 UTC 9 January (Fig. 6c) shows the cyclonic circulation associated with this feature. By this time the katabatic drainage onto Terra Nova Bay had ceased (Fig. 7). However, the regional analyses (see Fig. 6b–d) revealed that a second cold air mass over the Ross Ice Shelf spiralled in behind the subsynoptic-scale cyclone. This could have supported the continued development of L_1 once it arrived on the ice shelf. The source of this cold boundary-layer air mass could have been radiative cooling over the Ross Ice Shelf, katabatic drainage from East Antarctica through the glaciers that dissect the Transantarctic Mountains, and/or katabatic drainage from West Antarctica. The limited data preclude a definitive conclusion.

The next satellite image at 1332 UTC 9 January (not shown) showed the continued eastward displacement of L_1. At this time only a much weaker cloud signature was associated with L_6 indicating its weakening. On the next day, the satellite image at 0639 UTC 10 January (Fig. 2e) shows that L_1 was centred over the Ross Ice Shelf, but no evidence of L_6 was present. According to the sequence of satellite images available, L_1 exhibits its maximum development at 0639 UTC 10 January. The vortical cloud suggests that the subsynoptic-scale cyclone had a diameter of about 570 km (Fig. 2e), and the cloud-top temperatures which ranged between -27 and -30°C on the comma head and between -22 and -24°C on its tail indicate further development during the last 24 h. The maximum development of the vortex is confirmed by the AWS sea-level pressure analyses that showed that maximum intensity (strength) of the mesoscale cyclonic circulation occurred between 0300 UTC and 0900 UTC 10 January (as measured by the pressure difference between the outer closed isobar and the centre). The 500 hPa air temperature at McMurdo (obtained directly from the Australian 500 hPa charts) was -35°C on 10 January indicating that the top of the cloud was below the 500 hPa level, and that the associated midtropospheric circulation was probably confined below this level as well. The subsequent satellite images at 1321 UTC 10 January, 0447 UTC 11 January, and 0617 UTC 12 January indicate that the cloud signature associated with the cyclone started to weaken and to move into Marie Byrd Land where it disappeared some time on 13 January. The regional AWS analyses support this displacement (Fig. 6a–d) as do the synoptic-scale analyses (Fig. 3b–f) which show a trough moving eastward over the Ross Ice Shelf as the manifestation of the subsynoptic-scale cyclone.

Conceptual models

The classical Norwegian model of frontogenesis does not always explain the development of the satellite-observed cloud structure associated with cyclones (Reed 1990, Browning 1990). This has lead to the formulation of new conceptual models to describe the cloud structure and precipitation of extratropical cyclones based on the interaction of airflows that come from different air mass sources (Turner *et al.* 1993, Carlson 1980, Browning 1990). Because the cold air mass was supplied by the katabatic wind and

https://doi.org/10.1017/S0954102095000277 Published online by Cambridge University Press

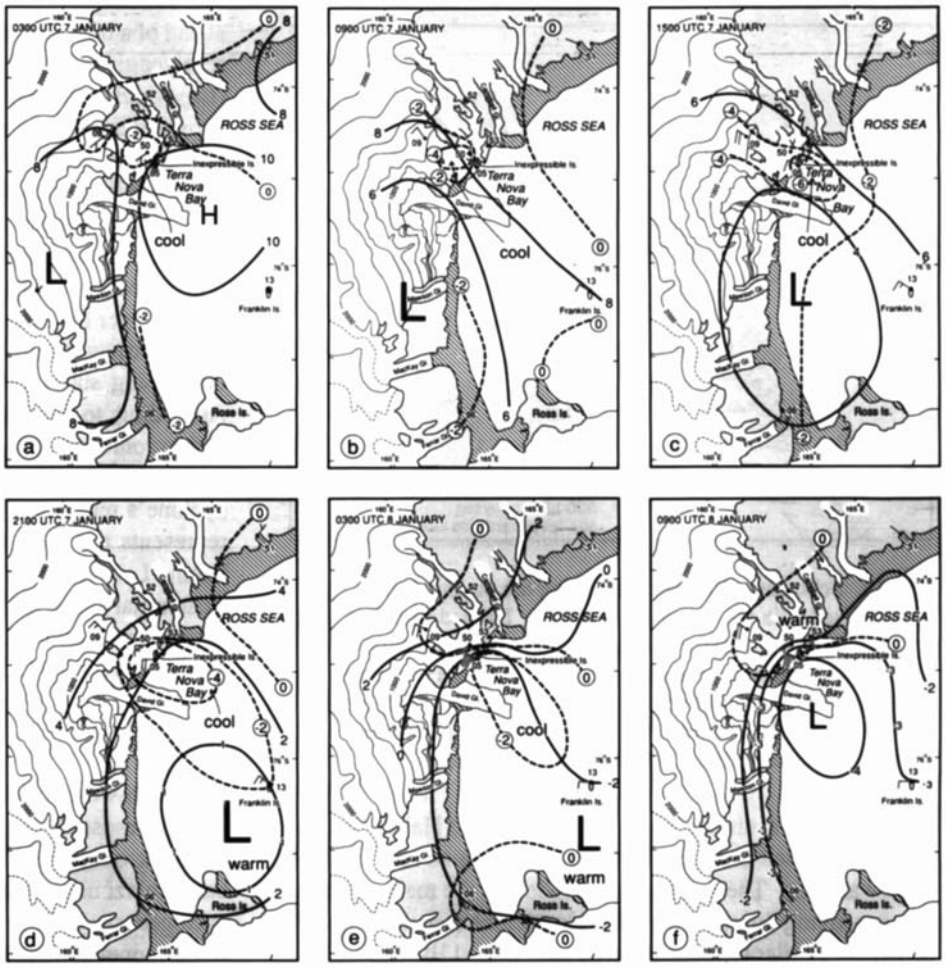

Fig. 8. Local analyses of pressure anomalies (solid lines) and potential temperatures in Celsius (dashed lines) along with wind directions and wind speeds at 6 h intervals from 0300 UTC 7 January to 0900 UTC 8 January 1988.

the formation of the cloud was induced by a pre-existing vortex, the development of the subsynoptic-scale cyclone discussed here may also be better described in terms of airflows. Fig. 11a–c are conceptual models suggested for the development of L_1 at 2100 UTC 7 January, 0339 UTC 8 January and 0639 UTC 10 January. The location of the surface front in Fig. 11b & c is the idealized position in relation to the cloud band (Anderson *et al.* 1973, fig. III 2.8). When the cyclonic circulation affected the south-western corner of the Ross Sea, relatively warmer air was absorbed into the circulation ahead of the centre. At the same time katabatic winds from Terra Nova Bay started to supply cold air into its north side (Fig. 11a & b, also see Fig. 9), forming the initial boundary-layer front. As the cyclone descended and increased its cyclonic vorticity, the cold boundary-layer air (warm air) cyclonically moved (ascended) around the centre of the vortex (Figs 9 & 11a). Once L_1 was over the northern edge of the Ross Ice Shelf, cold boundary layer air over the ice shelf spiralled in behind it (Figs 6c–d & 11c). The interaction of the warm and boundary-layer cold airflows further developed the initial low level cold front into a well-developed subsynoptic-scale system, as shown by the characteristics of the cloud signature (Fig. 2c–e). Turner *et al.* (1993) studied the development of a subsynoptic-scale vortex over the Weddell Sea. They concluded that the air motions associated with the

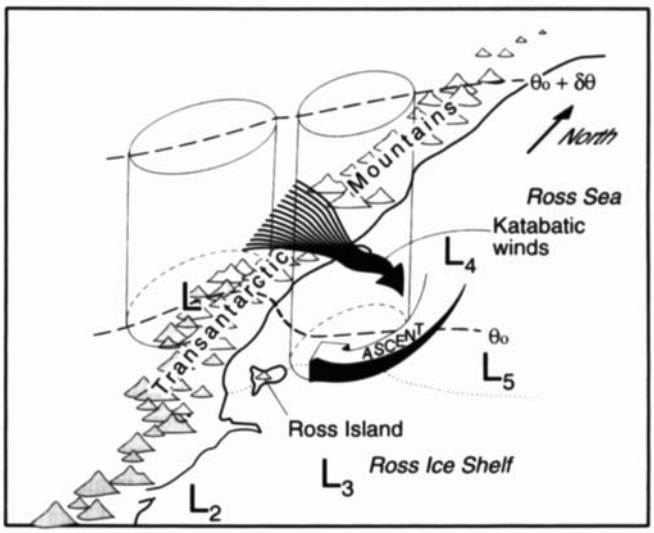

Fig. 9. Schematic illustration showing the mechanisms associated with the development of L1.θ_0 and $\theta_0 + \delta\theta$ are respectively near-surface and upper-level isentropes, not necessarily fixed boundaries.

https://doi.org/10.1017/S0954102095000277 Published online by Cambridge University Press

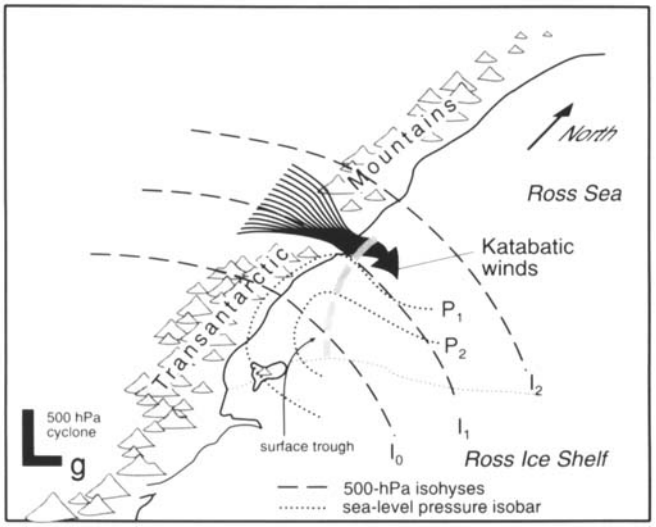

Fig. 10. Schematic illustration showing the mechanisms associated with the development of L6. Dashed lines I_0, I_1 and I_2 ($I_2 > I_1 > I_0$) are midtropospheric isohyses with cyclonic curvature, thin solid lines P_1 and P_2 ($P_1 > P_2$) are sea-level isobars, and thick dashed line locates the surface trough over the Ross Sea. Lg denotes the upper-level synoptic-scale cyclone located to the south-west of Ross Island.

vortex were cold air descending from inland of Halley Station into the Weddell Sea where it interacted with an area of low-level warm air. Their conceptual models of the main airflows accompanying the subsynoptic-scale cyclone (see their figs 13 & 14) are similar to those inferred here (Fig. 11b & c).

A more elaborate conceptual model that incorporates isentropic analysis has been developed by Browning and his colleagues (see Browning 1990); they introduced the concepts of *warm conveyor belt* (WCB) and *cold conveyor belt* (CCB) to respectively identify the warm and cold airflows within extratropical cyclones. We applied Browning's (1990) schematic portrayal (see his figs 8.9 & 8.16 for reference) of airflows to this subsynoptic-scale cyclone in the polar environment, to describe the interaction between a relatively warmer airflow originating over the Ross Sea and the cold boundary-layer air present over the Ross Ice Shelf. The well-developed frontal cloud signature observed on the satellite image at 0639 UTC 10 January (Fig. 2e) is used to infer the pattern of the airflows at this time. Fig. 12 illustrates the movement of the airflows associated with the frontal cloud in term of conveyor belts as described by Browning (1990). Once again, the location of the subsysnoptic-scale front is the idealized position in relation to the cloud band (Anderson *et al.* 1973, fig. III 2.8), but this time the system is treated as an occluded front. Because of the lack of upper-level data the conveyor belts are inferred solely on the basis of satellite imagery, and therefore we only intend to illustrate the possible airflows and not the complexity of the three-dimensional structure of the system. The solid arrow identifies a WCB with forward-sloping ascent relative to the movement of the front. As Browning (1990) pointed out such movement tends to occur ahead of a diffluent upper-level trough. The 500 hPa analyses resolved a synoptic-scale cyclone approaching McMurdo Station (Lg) which established a cyclonic midtropospheric circulation above the developing subsynoptic-scale cyclone. Because of the limited spatial resolution of these analyses, the details of the upper-level circulation cannot be deduced. The anticyclonic turn of the airflow may better explain the orientation and characteristics of the cloud at the frontal head. The dotted arrow is included to identify a CCB associated with a less cold air mass located over the eastern Ross Ice Shelf/Marie Byrd Land area that could have been absorbed into the cyclonic circulation as the developing subsynoptic-scale vortex moved south-eastward. According to Browing (1990) the CCB originated in the anticyclonic low-level flow to the south-east of the subsynoptic-scale cyclone. This flow moved westward in relation to the cyclone's movement and undercut the WCB. Dashed arrow represents the cold, dry boundary layer air that spiralled in behind L_1 (here called *boundary layer conveyor belt* (BLCB)). In summary, the WCB moved cyclonically southward while being lifted by the BLCB. Then it turned anticyclonically and ascended over the CCB.

Discussion

The south-western corner of the Ross Sea is a cyclogenetic area where mesoscale cyclones frequently form. A cold katabatic outbreak onto Terra Nova Bay can create a boundary-layer baroclinic zone establishing appropriate conditions for mesoscale cyclogenesis. The second cyclogenesis event (L_6), although weak, is one example of this. On the other hand, the development of L_1 points out that the south-western Ross Sea also provides the appropriate conditions for intensification of existing cyclonic perturbations that move into this region.

In this case, two factors contributed to the initial development of L_1: a) The cyclonic vorticity associated with the vortex increased as it descended from above 2000 m altitude to the Ross Sea; b) A cold katabatic outbreak occurred once the mesoscale cyclone was near Franklin Island supplying cold air to the north side of the cyclone. This cold air moved cyclonically around the centre of L_1, and would have interacted with relatively warm air from the Ross Sea trapped by the vortex, forming or enhancing a baroclinic front-like zone. A secondary cold air mass over the Ross Ice Shelf moved behind L_1 after 1200 UTC 8 January supporting its continued development.

The cyclonic circulation associated with the approach of the synoptic-scale upper-level cyclone, Lg, located to the west of the Ross Ice Shelf between 1200 UTC 7 January and 0000 UTC 11 January, could have supported the development of L_1 as well as the formation of L_6. However while L_1 developed into a major system, L_6 dissipated within the next 36 hours. This could have occurred because the cyclonic circulation of L_1 was strong enough to absorb L_6, and/or because of the different mechanisms involved in their development. The 500 hPa analyses indicate that the synoptic-scale upper-level cyclone (Lg) moved to the north-east of Ross Island sometime between 0000 and 1200

https://doi.org/10.1017/S0954102095000277 Published online by Cambridge University Press

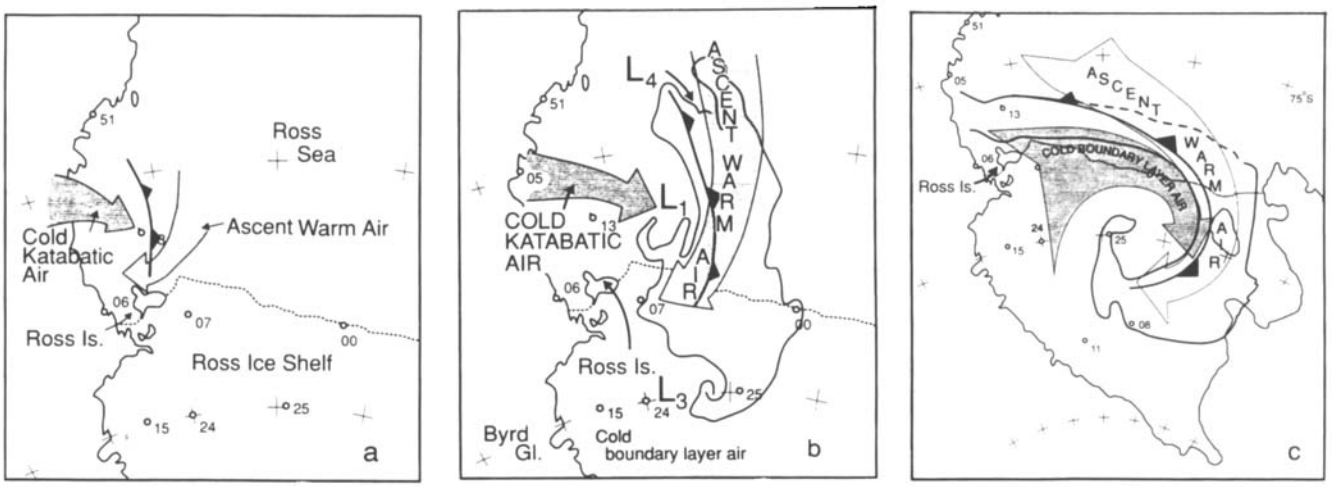

Fig. 11. Conceptual models of the airflows associated with the subsynoptic-scale vortex development at. **a.** 2100 UTC 7 January. **b.** 0339 UTC 8 January. **c.** 0639 UTC 10 January. In **b** and **c** the location of the front is the idealized position in relation to the cloud band (Anderson *et al.* 1973).

UTC 11 January and that later an upper-level ridge became established over the Ross Ice Shelf (Fig. 4f). The weakness of the subsynoptic-scale system from 11 January onward according to the satellite imagery, coincided with the north-west displacement of the upper-level synoptic-scale cyclone and with the subsequent establishment of the upper-level ridge.

Because the area under consideration is located immediately to the east of the high plateau of East Antarctica, the vertical winds at 850 hPa in the ECMWF (European Centre for Medium-Range Weather Forecasts) numerical analyses become too noisy to permit precise interpretation of the vertical motion field, and do not permit accurate calculation of the Q-vector field (Hoskins *et al.* 1978). On the other hand, evaluation of the diagnostic omega equation (Holton 1992, p.166–169) as was done for a mesoscale cyclogenesis case by Carrasco & Bromwich (1993) may lead here to erroneous results because the potential vorticity associated with the stretching of the subsynoptic-scale vortex seems to play a significant role. In fact, calculations yield lower tropospheric downward motion at the time when the cloud-top temperatures suggest upward motion. TOVS (Tiros Operational Vertical Sounder) data were available for only two satellite passages at 1715 UTC 7 January and 1653 UTC 8 January, after the downward movement of the subsynoptic-scale cyclone. Overall, the several geopotential thickness fields inferred from the TOVS data suggest warm (cold) air advection ahead (behind) the subsynoptic-scale vortex supporting the subsynoptic- and synoptic-scale descriptions inferred from conventional data. However, because of the uncertainty of TOVS data over the Antarctic continent and the lack of radiosonde data from McMurdo Station for direct comparison, these analyses are not presented here. In general, the lack of data, often found in the south polar region, precludes quantitative analysis for this event, and points out the importance of data collection programmes that will permit detailed analyses of similar cases in the future.

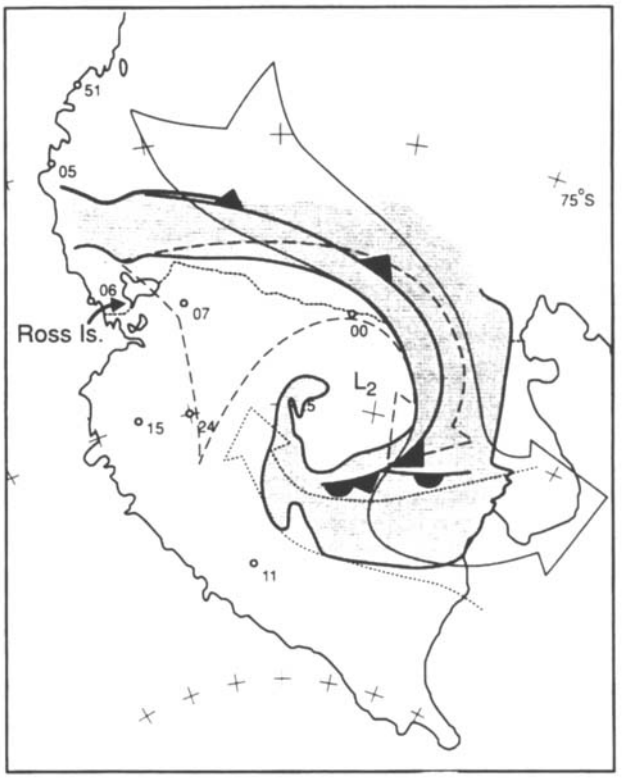

Fig. 12. Schematic illustration of the warm and cold airflows associated with the cloud organization at 0639 UTC 10 January (Fig. 2e), using Browning's (1990) conceptual model. The location of the front is the idealized position in relation to the cloud band (Anderson *et al.* 1973). Solid arrow = WCB, dotted arrow = CCB, and dashed arrow = BLCB.

The area to the north-east of the Ross Sea is known to be a cyclolysis region on the synoptic scale. Therefore, dissipating subsynoptic-scale cyclonic perturbations are likely to be found over the Ross Sea and Ross Ice Shelf. This raises the question

https://doi.org/10.1017/S0954102095000277 Published online by Cambridge University Press

as to what fraction of the mesoscale cyclones observed on satellite images or resolved by AWS regional analyses near Terra Nova Bay actually develop in this area and how many are pre-existing smaller vortices that move into the area and intensify. Resolution of this question will depend on the availability of good sequences of satellite data and a good array of AWS sites that together provide the necessary temporal and spatial resolution.

Acknowledgements

This research was sponsored by the Division of Polar Programs of the National Science Foundation through grants DPP-8816792 and DPP-9117448 to D.H. Bromwich. The satellite imagery was recorded by the U.S. Navy personnel at McMurdo Station, and obtained from Robert Whritner of the Arctic and Antarctic Research Center at Scripps Institution of Oceanography (NSF grant DPP-8815818). The satellite data were processed using the TeraScan software package developed by SeaSpace. Collection and distribution of the U.S. Antarctic AWS data are supported by the National Science Foundation grants DPP-8606385 and DPP-8818171 to Charles R. Stearns. Italian AWS data were made available to D.H. Bromwich by A. Pellegrini as a part of a collaborative effort with the Italian Antarctic Research Programme. We thank John Nagy for drafting the figures. This paper is Contribution 922 of the Byrd Polar Research Center.

References

Anderson, R.K., Ashman, J.P., Farr, G.R., Ferguson, E.W., Isayeva, G.N., Oliver, V.J., Parmenter, F.C., Popova, T.P., Skidmore, R.W., Smith, A.H. & Veltishchev, N.F. 1973. The use of satellite pictures in weather analysis and forecasting. (World Meteorological Organization). *Technical Note*, No. 124. 275 pp.

Bluestein, H.B. 1992. *Synoptic-Dynamic Meteorology in Midlatitudes, Volume I: Principles of Kinematics and Dynamics*. New York: Oxford University Press, 431pp.

Bromwich, D.H. 1987. A case study of mesoscale cyclogenesis over the south-western Ross Sea. *Antarctic Journal of United States*, **22**(5), 254-256.

Bromwich, D.H. 1989a. An extraordinary katabatic wind regime at Terra Nova Bay, Antarctica. *Monthly Weather Review*, **117**, 688-695.

Bromwich, D.H. 1989b. Subsynoptic-scale cyclone developments in the Ross Sea sector of the Antarctic. *In* Twitchell, P.F., Rasmussen, E.A. & Davidson, K.L. *eds. Polar and Arctic Lows*. Hampton: A. Deepak Publishing, 331-345.

Bromwich, D.H. 1991. Mesoscale cyclogenesis over south-western Ross Sea linked to strong katabatic winds. *Monthly Weather Review*, **119**, 1736-1752.

Bromwich, D.H. & Parish, T.R. 1988. Mesoscale cyclone interactions with the surface windfield near Terra Nova Bay, Antarctica. *Antarctic Journal of United States*, **23**(5), 172-175.

Bromwich, D.H., Parish, T.R. & Zorman, C.A. 1990. The confluence zone of the intense katabatic winds at Terra Nova Bay, Antarctica, as derived from airborne sastrugi surveys and mesoscale numerical modeling. *Journal of Geophysical Research*, **95**, 5496-5509.

Bromwich, D.H., Parish, T.R., Pellegrini, A., Stearns, C.R. & Weidner, G.A. 1993. Spatial and temporal characteristics of the intense katabatic winds at Terra Nova Bay, Antarctica. *Antarctic Research Series*, **61**, 47-68.

Browning, K.A. 1990. Organization of clouds and precipitation in extratropical cyclones. *In* Newton, C.W. & Holopainen, E.O. *eds. Extratropical cyclones: The Erik Palmén Memorial Volume*. Boston, Massachusetts: American Meteorological Society, 129-153.

Carlson, T.N. 1980. Airflow through midlatitude cyclones and the comma cloud pattern. *Monthly Weather Review*, **108**, 1498-1509.

Carrasco, J.F. & Bromwich, D.H. 1993. Mesoscale cyclogenesis dynamics over the south-western Ross Sea, Antarctica. *Journal of Geophysical Research*, **98**, 12973-12995.

Carrasco, J.F. & Bromwich, D.H. 1994. Climatological aspects of mesoscale cyclogenesis over the Ross Sea and Ross Ice Shelf regions of Antarctica. *Monthly Weather Review*, **122**, 2405-2425.

Guymer, L.B. 1986. Procedures and concepts used in Southern Hemisphere analyses at WMC Melbourne. *In Second International Conference on Southern Hemisphere Meteorology*. Boston: American Meteorological Society, 10-16.

Holton, J.R. 1992. *An introduction to dynamic meteorology*. San Diego: Academic Press, 511 pp.

Hoskins, B.J., Draghici, I., & Davies, H.C. 1978. A new look at the ω-equation. *Quarterly Journal of the Royal Meteorological Society*, **104**, 31-38.

Keller, L.M., Weidner, G.A., Stearns, C.R. & Sievers, M.F. 1989. *Antarctic automatic weather station data for the calendar year 1988*. Madison: Department of Meteorology, University of Wisconsin, 329 pp.

Parish, T.R. & Bromwich, D.H. 1987. The surface windfield over the Antarctic ice sheets. *Nature*, **328**, 51-54.

Parish, T.R. & Bromwich, D.H. 1989. Instrumented aircraft observations of the katabatic wind regime near Terra Nova Bay. *Monthly Weather Review*, **117**, 1570-1585.

Parish, T.R. & Bromwich, D.H. 1991. Continental-scale simulation of the Antarctic katabatic wind regime. *Journal of Climate*, **4**, 135-146.

Phillpot, H.R. 1991. The derivation of 500 hPa height from automatic weather station surface observations in the Antarctic continental interior. *Australian Meteorological Magazine*, **39**, 79-86.

Reed, R.J. 1990. Advances in knowledge and understanding of extratropical cyclones during the past quarter century: an overview. *In* Newton, C.W. & Holopainen, E.O. *eds. Extratropical cyclones: The Erik Palmén Memorial Volume*. Boston: American Meteorological Society, 27-45.

Schwerdtfeger, W. 1984. *Weather and Climate of the Antarctic*. New York: Elsevier, 261 pp.

Stearns, C.R. & Wendler, G. 1988: Research results from Antarctic automatic weather stations. *Review of Geophysics*, **26**, 45-61.

Streten, N.A, & Troup, A.J. 1973. A synoptic climatology of satellite-observed cloud vortices over the Southern Hemisphere. *Quarterly Journal of the Royal Meteorological Society*, **99**, 56-72.

Turner, J., Lachlan-Cope, T.A., Warren, D.E. & Duncan, C.N. 1993. A mesoscale vortex over Halley Station, Antarctica. *Monthly Weather Review*, **121**, 1317-1336.

Van Loon, H. 1972. Pressure in the Southern Hemisphere. *In* Newton C.W. *ed. Meteorology of the Southern Hemisphere*. Boston: American Meteorological Society, 59-86 pp.

Van Woert, M.L., Whritner, R.H., Waliser, D.E., Bromwich, D.H. & Comiso, J.C. 1992. ARC: A source of multisensor satellite data for polar science. *Eos, Transactions of the American Geophysical Union*, **73**(6), 65, 75-76.